Observation of η' Decays to $\pi^+\pi^-\pi^0$ and $\pi^+\pi^-e^+e^-$

P. Naik,[1] J. Rademacker,[1] D. M. Asner,[2] K. W. Edwards,[2] J. Reed,[2] A. N. Robichaud,[2] G. Tatishvili,[2] R. A. Briere,[3] H. Vogel,[3] P. U. E. Onyisi,[4] J. L. Rosner,[4] J. P. Alexander,[5] D. G. Cassel,[5] J. E. Duboscq,[5,*] R. Ehrlich,[5] L. Fields,[5] R. S. Galik,[5] L. Gibbons,[5] R. Gray,[5] S. W. Gray,[5] D. L. Hartill,[5] B. K. Heltsley,[5] D. Hertz,[5] J. M. Hunt,[5] J. Kandaswamy,[5] D. L. Kreinick,[5] V. E. Kuznetsov,[5] J. Ledoux,[5] H. Mahlke-Krüger,[5] D. Mohapatra,[5] J. R. Patterson,[5] D. Peterson,[5] D. Riley,[5] A. Ryd,[5] A. J. Sadoff,[5] X. Shi,[5] S. Stroiney,[5] W. M. Sun,[5] T. Wilksen,[5] S. B. Athar,[6] J. Yelton,[6] P. Rubin,[7] S. Mehrabyan,[8] N. Lowrey,[8] M. Selen,[8] E. J. White,[8] J. Wiss,[8] R. E. Mitchell,[9] M. R. Shepherd,[9] D. Besson,[10] T. K. Pedlar,[11] D. Cronin-Hennessy,[12] K. Y. Gao,[12] J. Hietala,[12] Y. Kubota,[12] T. Klein,[12] R. Poling,[12] A. W. Scott,[12] P. Zweber,[12] S. Dobbs,[13] Z. Metreveli,[13] K. K. Seth,[13] B. J. Y. Tan,[13] A. Tomaradze,[13] J. Libby,[14] L. Martin,[14] A. Powell,[14] G. Wilkinson,[14] H. Mendez,[15] J. Y. Ge,[16] D. H. Miller,[16] V. Pavlunin,[16] B. Sanghi,[16] I. P. J. Shipsey,[16] B. Xin,[16] G. S. Adams,[17] D. Hu,[17] B. Moziak,[17] J. Napolitano,[17] Q. He,[18] J. Insler,[18] H. Muramatsu,[18] C. S. Park,[18] E. H. Thorndike,[18] F. Yang,[18] M. Artuso,[19] S. Blusk,[19] S. Khalil,[19] J. Li,[19] R. Mountain,[19] K. Randrianarivony,[19] N. Sultana,[19] T. Skwarnicki,[19] S. Stone,[19] J. C. Wang,[19] L. M. Zhang,[19] G. Bonvicini,[20] D. Cinabro,[20] M. Dubrovin,[20] A. Lincoln,[20] and K. M. Ecklund[21]

(CLEO Collaboration)

[1]*University of Bristol, Bristol BS8 1TL, United Kingdom*
[2]*Carleton University, Ottawa, Ontario, Canada K1S 5B6*
[3]*Carnegie Mellon University, Pittsburgh, Pennsylvania 15213, USA*
[4]*Enrico Fermi Institute, University of Chicago, Chicago, Illinois 60637, USA*
[5]*Cornell University, Ithaca, New York 14853, USA*
[6]*University of Florida, Gainesville, Florida 32611, USA*
[7]*George Mason University, Fairfax, Virginia 22030, USA*
[8]*University of Illinois, Urbana-Champaign, Illinois 61801, USA*
[9]*Indiana University, Bloomington, Indiana 47405, USA*
[10]*University of Kansas, Lawrence, Kansas 66045, USA*
[11]*Luther College, Decorah, Iowa 52101, USA*
[12]*University of Minnesota, Minneapolis, Minnesota 55455, USA*
[13]*Northwestern University, Evanston, Illinois 60208, USA*
[14]*University of Oxford, Oxford OX1 3RH, United Kingdom*
[15]*University of Puerto Rico, Mayaguez, Puerto Rico 00681*
[16]*Purdue University, West Lafayette, Indiana 47907, USA*
[17]*Rensselaer Polytechnic Institute, Troy, New York 12180, USA*
[18]*University of Rochester, Rochester, New York 14627, USA*
[19]*Syracuse University, Syracuse, New York 13244, USA*
[20]*Wayne State University, Detroit, Michigan 48202, USA*
[21]*Rice University, Houston, Texas 77005, USA*

(Received 15 September 2008; published 11 February 2009)

Using $\psi(2S) \to \pi^+\pi^- J/\psi$, $J/\psi \to \gamma\eta'$ events acquired with the CLEO-c detector at the CESR e^+e^- collider, we make the first observations of the decays $\eta' \to \pi^+\pi^-\pi^0$ and $\eta' \to \pi^+\pi^- e^+e^-$, measuring absolute branching fractions $(37^{+11}_{-9} \pm 4) \times 10^{-4}$ and $(25^{+12}_{-9} \pm 5) \times 10^{-4}$, respectively. For $\eta' \to \pi^+\pi^-\pi^0$, this result probes the mechanism of isospin violation and the roles of $\pi^0/\eta/\eta'$-mixing and final state rescattering in strong decays. We also set upper limits on branching fractions for η' decays to $\pi^+\pi^-\mu^+\mu^-$, $2(\pi^+\pi^-)$, $\pi^+\pi^- 2\pi^0$, $2(\pi^+\pi^-)\pi^0$, $3(\pi^+\pi^-)$, and invisible final states.

DOI: 10.1103/PhysRevLett.102.061801 PACS numbers: 13.25.Jx, 13.20.Jf

Four decades after the first observation of the η' meson, its decays continue to provide a useful laboratory for probing strong interactions and new physics. Theoretical and experimental interest remains robust, in part because some expected modes have not yet been observed at all and some rare or forbidden modes have not been adequately limited. For example, of all possible multipion η' decays, only $\eta' \to 3\pi^0$ has been observed [1], and branching fraction limits for others are not stringent, lying in the range of (1%–9%) [2–5]. No η' decays with an e^+e^- in the final state have been seen, and just one with a dimuon ($\eta' \to \gamma\mu^+\mu^-$) has been measured. New physics would

be indicated by invisible decays $\eta' \to \mathcal{I}$, i.e., decays that leave no trace in any detector because they are composed of weakly interacting particles such as light dark matter. BES [6] has set the only such limit, $\mathcal{B}(\eta' \to \mathcal{I}) < 14 \times 10^{-4}$ at 90% confidence level (C.L.).

Decay rates for three-pion decays of η' are commonly expressed relative to their respective $\pi\pi\eta$ branching fractions because they could arise from η-π^0 mixing: $r_0 \equiv \mathcal{B}(\eta' \to 3\pi^0)/\mathcal{B}(\eta' \to \pi^0\pi^0\eta) = (75 \pm 13) \times 10^{-4}$ [7] and $r_\pm \equiv \mathcal{B}(\eta' \to \pi^+\pi^-\pi^0)/\mathcal{B}(\eta' \to \pi^+\pi^-\eta)$. The decay $\eta' \to \pi^+\pi^-\pi^0$ has garnered attention [5,8–10] both because experimental limits [2–5] are large and because its rate can probe isospin symmetry breaking. Under the two assumptions that $\pi^+\pi^-\pi^0$ appears only through $\eta' \to \pi^+\pi^-\eta$ followed by η-π^0 mixing and that such decays populate the available phase space uniformly, $r_\pm$ is found to be proportional to the light quark mass difference $(m_u - m_d)$ [11] and implies $r_\pm/r_0 \simeq 0.37$ [12]. Suggesting neither assumption is justified, Ref. [12] employs the framework of $U(3)$ chiral effective field theory [13] to examine η' decays. The incorporation of measured [14] $\eta' \to \pi\pi\eta$ Dalitz slope parameters implies a large contribution to $\eta' \to \pi^+\pi^-\pi^0$ from final state rescattering: the prediction is that $r_\pm/r_0 \simeq 5$ and that dramatic structure should be present in the $\pi^+\pi^-\pi^0$ Dalitz plot.

Branching fractions for $\eta' \to l^+l^-X$ ($\ell^\pm \equiv e^\pm, \mu^\pm$) are expected to scale with those for $\eta' \to \gamma X$; the most copious dileptonic decay should be $\eta' \to \pi^+\pi^-e^+e^-$. Since other π^0 and η decays to e^+e^-X occur at $\simeq$1% [7] of the corresponding γX decay, $\mathcal{B}(\eta' \to \pi^+\pi^-e^+e^-) \simeq 0.3\%$ is expected. Two different theoretical approaches [15,16] both predict $\mathcal{B}(\eta' \to \pi^+\pi^-e^+e^-) \simeq 0.2\%$, ρ^0-dominance for the $\pi^+\pi^-$, and an e^+e^- mass distribution peaking just above $2m_e$ but with a long tail extending to $\simeq 300$ MeV. The experimental limit is $\mathcal{B}(\eta' \to \pi^+\pi^-e^+e^-) < 0.6\%$ [17]. The corresponding dimuon channel is expected to be much rarer, with predictions of $\mathcal{B}(\eta' \to \pi^+\pi^-\mu^+\mu^-) \simeq 2 \times 10^{-5}$ [15,16] and no experimental limit extant.

In this Letter we search for decays of the η' meson to eight final states: $\pi^+\pi^-\pi^0$, $\pi^+\pi^-e^+e^-$, $\pi^+\pi^-\mu^+\mu^-$, $2(\pi^+\pi^-)$, $3(\pi^+\pi^-)$, $2(\pi^+\pi^-)\pi^0$, $\pi^+\pi^-2\pi^0$, and $\mathcal{I}$. Yields are normalized using the well-established decay chain $\eta' \to \pi^+\pi^-\eta$, $\eta \to \gamma\gamma$, hereafter denoted as $\eta' \to \pi^+\pi^-\eta[\gamma\gamma]$, which was successfully used in a recent CLEO measurement [18] of the η' mass and found to provide a virtually background-free event sample. Events were acquired at the CESR e^+e^- collider with the CLEO detector [19], mostly in the CLEO-c configuration (95%), with the balance from CLEO III. The data sample corresponds to 27×10^6 [20] produced $\psi(2S)$ mesons, of which about 4×10^4 decay as $\psi(2S) \to \pi^+\pi^-J/\psi$, $J/\psi \to \gamma\eta'$.

For all the exclusive decay modes (i.e., all but invisible), event selection requires finding every particle in the decay. The tracking system must find exactly two oppositely-charged particles for the transition dipion, and two, four, or six more tracks of net charge zero, allowing for multiple combinations per event (which tends not to occur). Photon candidates must have energy exceeding 37 MeV, and either be more than 30 cm from any shower associated with one of the charged pions, or, when between 15 and 30 cm from such a shower, have a photonlike lateral shower profile. Showers are rejected as photon candidates if they lie near the projection of any charged pion's trajectory into the calorimeter, or align with the initial momentum of any $\pi^\pm$ candidate within 100 mrad. Photon candidates are ordered by energy, with the most energetic always taken as the radiative photon from the J/ψ, and subsequent ones, if required, must be taken as from the η'. That is, a shower can be included in the decay chain only if every other photon of higher energy has also been used. Photon pairs are candidates for a π^0 or η if their invariant mass satisfies $M(\gamma\gamma) = 115$–150 MeV or 500–580 MeV, respectively, and are then constrained to the known π^0 or η masses [7].

All decay products are constrained to originate from a single point (vertex) consistent with the beam spot. The vertex-constrained event is additionally constrained to the known $\psi(2S)$ mass [7] and three-momentum, including the effect of the $\simeq 3$ mrad crossing angle of the e^+ and e^- beams. Quality restrictions are applied to both the vertex (χ^2_V/d.o.f. < 10) and full event four-momentum (χ^2_E/d.o.f. < 10) kinematic fits. From this point onward, all selections are based upon the four-momenta obtained from the kinematic fit so as to improve resolutions. The mass recoiling against the $\psi(2S)$-to-J/ψ transition dipion must lie in the range 3092–3102 MeV. The invariant mass of the η' candidate, $M(\eta')$, must lie in the window 952–964 MeV. For the exclusive modes [$\eta' \to \mathcal{I}$], sidebands in $M(\eta')$ [E^*_γ] are used to extrapolate a linear background level into the signal region. Sideband intervals are, for $M(\eta')$, 916–940 or 976–1000 MeV, and, for E^*_γ, 1220–1320 or 1460–1560 MeV.

Candidates for $\pi^+\pi^-e^+e^-$ are additionally required to have an e^+e^- invariant mass $M(e^+e^-)$ below 100 MeV and which lies outside a window of 8–25 MeV, as well as to pass a tighter vertexing criterion, χ^2_V/d.o.f. < 3. These restrictions act to suppress feed-across from $\eta' \to \pi^+\pi^-\gamma$ when the photon converts in the material in the vacuum pipe or detectors. In such events the conversion electrons vertex poorly with the other tracks and the beam spot. When forced to form a common vertex with other tracks, $M(e^+e^-)$ tends to be in the window 8–25 MeV due to the the discrete locations of the material. Similar restrictions were used effectively in Ref. [21] in the selection of $\eta \to \gamma e^+e^-$ events.

No lepton identification is required for $\pi^+\pi^-e^+e^-$ or $\pi^+\pi^-\mu^+\mu^-$ candidate events. Instead, all combinations of pion and lepton mass assignments are made to the four charged particles assigned to be the η' decay products, and only those satisfying the respective kinematic fit are re-

tained. Background from $\pi^+\pi^-\gamma$ conversions with incorrectly swapped mass assignments (i.e., when a pion is mistakenly assigned the electron mass and an electron the pion mass) are suppressed by the $M(e^+e^-) < 100$ MeV requirement; the $M(e^+e^-) = 8$–25 MeV veto eliminates conversion background with correct mass assignments.

Candidates for $\eta' \to \pi^+\pi^-\pi^0$ are additionally required to pass a more restrictive criterion for the four-momentum fit of $\chi^2_E/\text{d.o.f.} < 3$ to suppress feed-across from $\eta' \to \pi^+\pi^-\gamma$, which fakes $\pi^+\pi^-\pi^0$ when a shower from a pion interaction in the calorimeter is erroneously taken as a photon candidate and happens to form a π^0 candidate with the real photon from the η' decay. For $\pi^+\pi^-2\pi^0$, the four-momentum fit must have $\chi^2_E/\text{d.o.f.} < 3$ to suppress background from other J/ψ decays. For $\eta' \to (2, 3)(\pi^+\pi^-)$, the photon from the J/ψ decay may not pair with any other photon candidate in the event to form a π^0 or η so as to suppress backgrounds from $J/\psi \to (2, 3)(\pi^+\pi^-)(\pi^0/\eta)$. To reduce feedacross from $\eta' \to \pi^+\pi^-\eta[\pi^+\pi^-\pi^0]$ into $\eta' \to 2(\pi^+\pi^-)\pi^0$, candidates must not contain a three-pion combination that satisfies a constraint to the η mass with $\chi^2_M/\text{d.o.f.} < 10$. The sum of all unused photon candidates' energies cannot exceed 75 MeV for $\pi^+\pi^-2\pi^0$ in order to suppress backgrounds with higher neutral multiplicities.

Candidates for I decays are subject to a simpler set of criteria. Exactly two charged particles of opposite charge can be found in the event, and their recoil mass must lie in the same window as the exclusive decays. Signal events would have a monochromatic photon in the J/ψ rest frame, so we require that the most energetic photon candidate must, when boosted into the J/ψ center-of-mass using the dipion momentum, have energy $E^*_\gamma = 1340$–1440 MeV. The sum of all unused photon candidates' energies must be less than 75 MeV. The above restrictions on excess charged and neutral energy are evaded by events in which the particles recoiling against the transition dipion and radiative photon do not enter the active fiducial volume of the detector; hence we require that the missing momentum must have $|\cos\theta| < 0.7$, assuring the rejection of such events. Background from $J/\psi \to \bar{n}n$ in which the neutron is undetected and the antineutron shower has energy in the signal window is suppressed by requiring the radiative photon to have a lateral profile consistent with that of an electromagnetic shower.

Efficiencies for signal and feed-across from other η' decays are modeled with Monte Carlo (MC) samples that were generated using the EVTGEN event generator [22], fed through a GEANT-based [23] detector simulation, and subjected to event selection criteria. All η' decays are generated using phase space, except that for $\pi^+\pi^-l^+l^-$ and $\pi^+\pi^-\gamma$ we assume the dipion to come from a ρ^0, and the $M(l^+l^-)$ distributions have been tuned to match those of Ref. [16]. For invisible decays we use $\eta' \to \nu\bar{\nu}$.

The data exhibit signals for $\eta' \to \pi^+\pi^-\pi^0$ (24 events) and $\eta' \to \pi^+\pi^-e^+e^-$ (8 events), with predicted background levels of 3.8 and 0.14 events, respectively. Distributions in $M(\eta')$ appear in Fig. 1. The signal level and corresponding 68% C.L. interval in each case are obtained by subtracting the estimated background and accounting for the statistics of signal- and sideband-region data as well as that of $\eta' \to \pi^+\pi^-\gamma$ MC samples using a procedure similar to that of Ref. [24]. We consider two sources of background, one peaking in the signal region (from other η' decays, in these two cases the only significant channel being $\eta' \to \pi^+\pi^-\gamma$, normalized by branching fractions [7] relative to $\eta' \to \pi^+\pi^-\eta[\gamma\gamma]$) and the second linear across the mass region. The former is estimated from a MC sample to be 1.3 events for $\pi^+\pi^-\pi^0$ and 0.14 events for $\pi^+\pi^-e^+e^-$, and the latter from the mass sidebands to be 2.5 and 0 events, respectively. For $\pi^+\pi^-e^+e^-$, the two events between the signal and sideband regions are consistent with tails of the signal.

Statistical significance for each signal is obtained from a large ensemble of simulated trials in which the backgrounds are thrown as appropriately-scaled Poisson distributions and the fraction of such trials in which the number

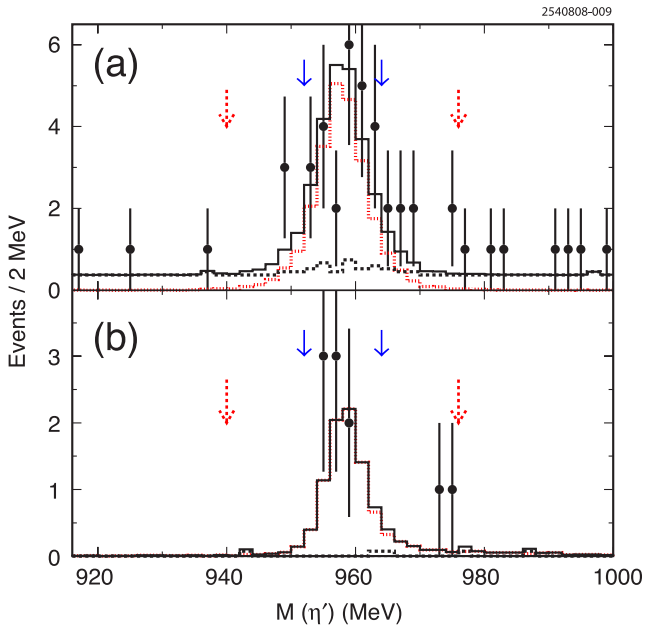

FIG. 1 (color online). Distributions in $M(\eta')$ for (a) $\eta' \to \pi^+\pi^-\pi^0$ and (b) $\eta' \to \pi^+\pi^-e^+e^-$. Solid circles represent data (nonzero bin entries only), the dashed histogram is the sum of a linear background normalized to the sideband populations in data and feedacross from $\eta' \to \pi^+\pi^-\gamma$ normalized by branching fraction, the dotted histogram is the signal MC shape normalized to the observed signal level, and the solid line is the sum of dotted and dashed histograms. Solid (dashed) arrows indicate nominal signal (sideband) region boundaries; sidebands extend to the edges of the plots. All selection criteria are applied here except to $M(\eta')$.

of events meets or exceeds that of the data is determined. In both cases the significances exceed 6σ.

The number of events in the normalization mode, $\eta' \to \pi^+\pi^-\eta[\gamma\gamma]$, is evaluated in an identical manner as our signal modes, and has no appreciable peaking feedacross background; nonpeaking backgrounds lead to a 0.2% overall subtraction. The absolute number of $\eta' \to \pi^+\pi^-\eta[\gamma\gamma]$ events is compatible with that expected from the size of our data sample, the MC efficiency for this mode, and PDG branching fractions [7].

Figure 2 shows kinematic distributions for $\eta' \to \pi^+\pi^-\pi^0$ and $\pi^+\pi^-e^+e^-$; within the statistical precision of so few events, we observe consistency of the data with the MC predictions. In Fig. 2(a) the $\gamma\gamma$ mass distribution for the π^0 candidate in $\eta' \to \pi^+\pi^-\pi^0$ verifies the cleanliness of that sample. Of particular interest for the $\eta' \to \pi^+\pi^-\pi^0$ decay is the Dalitz plot distribution shown in Fig. 2(b) and 2(c), where data and phase-space MC simulation are shown side by side (these can be compared to the prediction in Fig. 1 of Ref. [12]). We compare the Dalitz plot population density of data points to the two predictions and find much better agreement with the phase-space model than with that of rescattering through $\rho^\pm$ [12]. The E^*_γ distribution for $\eta' \to \mathcal{I}$ appears in Fig. 3 and shows no indication of a signal. For the channels where no signals are apparent, we compute 90% C.L. upper limits on the signal yields.

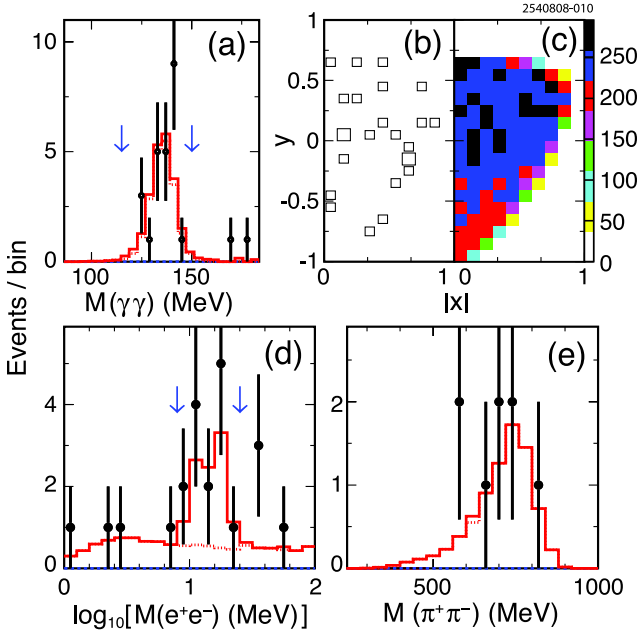

FIG. 2 (color online). Distributions in (a) the invariant mass of the two photons in the π^0 candidate in $\eta' \to \pi^+\pi^-\pi^0$; (b) Dalitz variables y vs $|x|$ for $\eta' \to \pi^+\pi^-\pi^0$ (uncorrected for efficiency) for data, where box absence or size indicates 0, 1, or 2 events in each 0.1-by-0.1 bin, and (c) from a phase-space MC simulation, where bin shading indicates relative population; (d) the e^+e^- invariant mass for $\eta' \to \pi^+\pi^-e^+e^-$; (e) the $\pi^+\pi^-$ invariant mass for $\eta' \to \pi^+\pi^-e^+e^-$. In (a), (d), and (e), solid circles represent the data, the dotted histogram is the MC signal shape normalized to the yields found in Table I, and the solid line is the sum of MC signal and predicted $\eta' \to \pi^+\pi^-\gamma$ feedacross. The region between the arrows indicates the selected region in (a) and an excluded region in (d). All selection criteria, including that upon $M(\eta')$, are applied here, except to $M(\gamma\gamma)$ in (a) and to $M(e^+e^-)$ in (d). The quantities x and y are defined as $x \equiv \sqrt{3}(T_+ - T_-)/Q$, $y \equiv (3T_0/Q) - 1$, T_0 ($T_\pm$) is the π^0 ($\pi^\pm$) kinetic energy in the η' center of mass, and $Q \equiv T_0 + T_+ + T_-$.

Table I displays the numerical results for each mode. No data events within the $M(\eta')$ signal window are seen for the modes $\pi^+\pi^-\mu^+\mu^-$, $2(\pi^+\pi^-)$, or $3(\pi^+\pi^-)$; for $2(\pi^+\pi^-)\pi^0$ we find one signal event with 0.5 background, and for $\pi^+\pi^-2\pi^0$, 5 signal events with 2 background. The production rate R of each mode relative to that of $\eta' \to \pi^+\pi^-\eta[\gamma\gamma]$ is defined as $R \equiv [\mathcal{B}(\eta' \to X)/\mathcal{B}(\eta' \to \pi^+\pi^-\eta) \times \mathcal{B}(\eta \to \gamma\gamma)]$, and the absolute branching fraction $B \equiv \mathcal{B}(\eta' \to X)$. R is obtained by dividing the yield by its efficiency relative to the normalization mode and the number of events in the normalization mode; B is obtained from R by multiplying it by (0.1753 ± 0.0056), the value of the denominator in R using branching fractions compiled in Ref. [7]. Overall normalizations cancel in the values of R, as do some of the track- and photon-finding systematic errors, depending upon mode. Systematic errors include detector modeling, the background linearity assumption, and the possible presence of intermediate resonances, amounting to 10%–20%, depending upon mode; however, statistical errors dominate the systematic uncertainties here. The final column shows previous measurements, if any, for each mode: our measurements provide the first limits for $\eta' \to \pi^+\pi^-\mu^+\mu^-$ and $\pi^+\pi^-2\pi^0$ and improve upon those for the other modes.

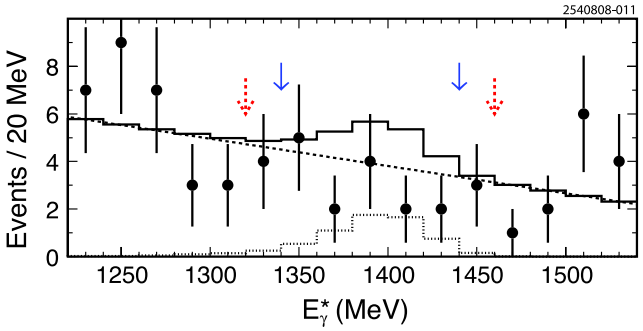

FIG. 3 (color online). Distribution of E^*_γ (see text) for $J/\psi \to \gamma\eta'$, $\eta' \to \mathcal{I}$ candidate events. Solid circles represent data (nonzero bin entries only), the dashed histogram is the linear background normalized to the sideband populations in data, the dotted histogram is the signal MC shape normalized to the 90% C.L. upper limit, and the solid line is the sum of dotted and dashed histograms. Solid (dashed) arrows indicate nominal signal (sideband) region boundaries; sidebands extend to the edges of the plot. All selections are applied here except to E^*_γ.

TABLE I. Results for $\eta' \to X$ search, showing for each mode X the efficiency relative to that of the normalization mode $\eta' \to \pi^+\pi^-\eta[\gamma\gamma]$, ϵ/ϵ_0; the net number of signal events, after background subtractions, N (or 90% C.L. upper limit where indicated with "<"); the branching fraction ratio R [see text]; the absolute branching fraction $B \equiv \mathcal{B}(\eta' \to X)$ and its previous upper limit P [7]. Entries for R and B include systematic errors.

Mode X	ϵ/ϵ_0	N	$R(10^{-3})$	$B(10^{-4})$	$P(10^{-4})$
$\pi^+\pi^-\eta[\gamma\gamma]$	1.00	1756 ± 42	$\cdots$	$\cdots$	$\cdots$
$\pi^+\pi^-\pi^0$	0.55	$20.2^{+6.1}_{-4.8}$	$21^{+6}_{-5} \pm 2$	$37^{+11}_{-9} \pm 4$	<500
$\pi^+\pi^-e^+e^-$	0.31	$7.9^{+3.9}_{-2.7}$	$14^{+7}_{-5} \pm 3$	$25^{+12}_{-9} \pm 5$	<60
$\pi^+\pi^-\mu^+\mu^-$	2.14	<4.8	<1.3	<2.4	$\cdots$
$2(\pi^+\pi^-)$	1.02	<2.3	<1.4	<2.4	<100
$\pi^+\pi^-2\pi^0$	0.18	<4.1	<15	<27	$\cdots$
$2(\pi^+\pi^-)\pi^0$	0.21	<3.6	<11	<20	<100
$3(\pi^+\pi^-)$	0.47	<2.3	<3.0	<5.3	<100
Invisible	0.74	<5.8	<5.4	<9.5	<14

In conclusion, we report the first observation of the decays $\eta' \to \pi^+\pi^-\pi^0$ and $\eta' \to \pi^+\pi^-e^+e^-$ and measurement of their branching fractions. We find $\mathcal{B}(\eta' \to \pi^+\pi^-\pi^0) = (37^{+11}_{-9} \pm 4) \times 10^{-4}$ and $r_\pm = (83 \pm 22) \times 10^{-4}$. Using the branching fractions of Ref. [7], we determine $r_\pm/r_0 = 1.11 \pm 0.35$, more than 2 standard deviations above the π^0-η-mixing prediction of 0.37, and far below the chiral unitary framework prediction of 5 [12]. The dileptonic results $\mathcal{B}(\eta' \to \pi^+\pi^-e^+e^-) = (25^{+12}_{-9} \pm 5) \times 10^{-4}$ and $\mathcal{B}(\eta' \to \pi^+\pi^-\mu^+\mu^-) < 2.4 \times 10^{-4}$ are consistent with predictions [15,16]. We also obtain first or improved branching fraction upper limits for η' decays to multipion and invisible final states.

We gratefully acknowledge the effort of the CESR staff in providing us with excellent luminosity and running conditions. This work was supported by the A. P. Sloan Foundation, the National Science Foundation, the U. S. Department of Energy, the Natural Sciences and Engineering Research Council of Canada, and the U.K. Science and Technology Facilities Council.

*Deceased.

[1] D. Alde *et al.*, Yad. Fiz. **47**, 385 (1988) [Sov. J. Nucl. Phys. **47**, 243 (1988)]; F. G. Binon *et al.*, Phys. Lett. B **140**, 264 (1984).
[2] Ref. [3] quotes $\mathcal{B}(\eta' \to \pi^+\pi^-\pi^0) < 9\%$. Ref. [4] quotes $\mathcal{B}(\eta' \to \pi^+\pi^-\pi^0) < 5\%$, but is unpublished. VES [5] has reported an upper limit $\mathcal{B}(\eta' \to \pi^+\pi^-\pi^0) < 1.75\%$, but it is a preliminary conference result.
[3] J. S. Danburg *et al.*, Phys. Rev. D **8**, 3744 (1973).
[4] A. Rittenberg, Ph.D. thesis 1969 (unpublished); http://repositories.cdlib.org/lbnl/UCRL-18863.
[5] V. Nikolaenko *et al.* (VES Collaboration), AIP Conf. Proc. **796**, 154 (2005).
[6] M. Ablikim *et al.* (BES Collaboration), Phys. Rev. Lett. **97**, 202002 (2006).
[7] C. Amsler *et al.* (Particle Data Group), Phys. Lett. B **667**, 1 (2008).
[8] H. H. Adam *et al.* (WASA-at-COSY Collaboration), arXiv:nucl-ex/0411038; M. J. Zielinski, arXiv: 0807.0576v1.
[9] C. Bloise, AIP Conf. Proc. **950**, 192 (2007).
[10] A. Thomas, AIP Conf. Proc. **950**, 198 (2007).
[11] D. J. Gross, S. B. Treiman, and F. Wilczek, Phys. Rev. D **19**, 2188 (1979).
[12] B. Borasoy, U.-G. Meissner, and R. Nissler, Phys. Lett. B **643**, 41 (2006).
[13] B. Borasoy and R. Nissler, Eur. Phys. J. A **26**, 383 (2005).
[14] V. Dorofeev *et al.* (VES Collaboration), Phys. Lett. B **651**, 22 (2007).
[15] A. Faessler, C. Fuchs, and M. I. Krivoruchenko, Phys. Rev. C **61**, 035206 (2000).
[16] B. Borasoy and R. Nissler, Eur. Phys. J. A **33**, 95 (2007).
[17] A. Rittenberg and G. R. Kalbfleisch, Phys. Rev. Lett. **15**, 556 (1965).
[18] J. Libby *et al.* (CLEO Collaboration), Phys. Rev. Lett. **101**, 182002 (2008).
[19] Y. Kubota *et al.* (CLEO Collaboration), Nucl. Instrum. Methods Phys. Res., Sect. A **320**, 66 (1992); M. Artuso *et al.*, Nucl. Instrum. Methods Phys. Res., Sect. A **554**, 147 (2005); D. Peterson *et al.*, Nucl. Instrum. Methods Phys. Res., Sect. A **478**, 142 (2002); CLEO-c/CESR-c Taskforces & CLEO-c Collaboration, Cornell University LEPP Report No. CLNS 01/1742, 2001 (unpublished).
[20] H. Mendez *et al.* (CLEO Collaboration), Phys. Rev. D **78**, 011102 (2008).
[21] A. Lopez *et al.* (CLEO Collaboration), Phys. Rev. Lett. **99**, 122001 (2007).
[22] D. J. Lange, Nucl. Instrum. Methods Phys. Res., Sect. A **462**, 152 (2001).
[23] R. Brun *et al.*, GEANT 3.21, CERN Program Library Long Writeup W5013, 1993 (unpublished).
[24] G. J. Feldman and R. D. Cousins, Phys. Rev. D **57**, 3873 (1998).